Sustainable Chemistry

Deutsche Ausgabe: DOI: 10.1002/ange.201602226
Internationale Ausgabe: DOI: 10.1002/anie.201602226

Importance of Micropore–Mesopore Interfaces in Carbon Dioxide Capture by Carbon-Based Materials

Gema Durá, Vitaliy L. Budarin, José A. Castro-Osma, Peter S. Shuttleworth, Sophie C. Z. Quek, James H. Clark, and Michael North**

Abstract: *Mesoporous carbonaceous materials (Starbons®) derived from low-value/waste bio-resources separate CO_2 from CO_2/N_2 mixtures. Compared to Norit activated charcoal (AC), Starbons® have much lower microporosities (8–32 % versus 73 %) yet adsorb up to 65 % more CO_2. The presence of interconnected micropores and mesopores is responsible for the enhanced CO_2 adsorption. The Starbons® also showed three–four times higher selectivity for CO_2 adsorption rather than N_2 adsorption compared to AC.*

Separation of CO_2 from other gases is a key part of technological processes in the energy sector. Thus, post-combustion carbon capture relies on the separation of CO_2 from the other components of flue gas (predominantly N_2),[1] whilst purification of natural gas from landfill, biogas plants or some gas-fields relies on the separation of CO_2 from the combustible components of natural gas (predominantly CH_4).[2] Methods to capture CO_2 include: chemical absorption, physical adsorption, cryogenic separation and membrane separation.[3] Adsorption-based methods such as pressure-swing, vacuum-swing, and temperature-swing adsorption, are the most promising technologies for CO_2 capture because of the low costs, controllability, simplicity, low energy demand, high adsorption capacity, and easy regeneration of the adsorbents. Porous materials which have been studied as adsorbents include: zeolites,[4] activated carbon,[5] and metal–organic frameworks (MOFs).[6] Of these, carbon-based materials have the advantages of fast adsorption/desorption kinetics, high surface area, large pore volume, low density, reusability, minimal costs, potentially environmentally benign nature, chemical inertness, and high thermal stability.

The Clark group has developed a template-free route to obtain mesoporous materials from abundant, renewable waste resources such as starch or alginic acid, leading to mesoporous carbons known as Starbons®.[7] These materials have been shown to have applications in areas including: catalysis, dye adsorption, and chromatographic separation. Established wisdom[8] is that microporous solids (preferably with pore diameters less than 0.8 nm[8a]) are optimal for gas separation, so mesoporous carbons such as Starbon® would not be expected to perform well in this application. Never the less, we decided to investigate the application of these materials to CO_2 separation.

The nature of Starbons® (e.g. functional groups present, surface area, average pore radius) varies depending on the temperature at which the polysaccharide is carbonized and the characterization of these materials has been reported previously.[7] Therefore, a range of Starbons® were prepared as previously reported[7] with carbonization temperatures of 300 to 1200 °C and are herein referred to as S300, A1200 and so forth depending on their parent material (starch or alginic acid). FTIR, Raman, and solid-state NMR spectra along with combustion analysis data and SEM images for these materials is given in the Supporting Information and shows that as the carbonization temperature increases to 600–800 °C, the materials dehydrate and become more graphitic in nature. As a reference material we chose commercially available Norit activated carbon (AC) which is a widely used microporous form of carbon.[9] The surface area, pore volume, and pore radius of all the materials were determined by porosimetry with N_2 at 77 K (Table 1) and the resulting adsorption

Table 1: Porosimetry data for the carbonaceous materials used in this work.

Material	S_{BET} [$m^2 g^{-1}$]	V_{total} [$cm^3 g^{-1}$]	$V_{micropore}$ [$cm^3 g^{-1}$]	Percentage of micropores	Average pore radius [nm]
AC	798	0.6	0.42	73.4	2.1
S300	241	1.1	0.09	8.1	19.7
S450	448	1.3	0.21	16.6	22.2
S650	826	1.3	0.39	30.0	16.3
S800	895	1.3	0.40	31.9	12.4
S1000	862	1.3	0.39	29.7	14.7
S1200	678	1.4	0.30	21.0	17.5
A300	304	1.2	0.14	11.6	8.6
A550	500	1.0	0.23	23.0	6.9
A800	931	1.4	0.39	27.7	5.9
A1000	675	1.4	0.27	18.5	6.4
A1200	427	1.1	0.16	13.9	6.3

[*] Dr. G. Durá, Dr. V. L. Budarin, S. C. Z. Quek, Prof. J. H. Clark, Prof. M. North
Green Chemistry Centre of Excellence
Department of Chemistry, The University of York
York, YO10 5DD (UK)
E-mail: james.clark@york.ac.uk
michael.north@york.ac.uk
Dr. J. A. Castro-Osma
Universidad de Castilla-La Mancha
Departamento de Química Inorgánica
Orgánica y Bioquímica-Centro de Innovación en
Química Avanzada (ORFEO-CINQA)
Instituto Regional de Investigación Científica Aplicada-IRICA
13071 Ciudad Real (Spain)
Dr. P. S. Shuttleworth
Departamento de Física de Polímeros
Elastómeros y Aplicaciones Energéticas
Instituto de Ciencia y Tecnología de Polímeros, CSIC
c/Juan de la Cierva 3, 28006 Madrid (Spain)

Supporting information for this article can be found under: http://dx.doi.org/10.1002/anie.201602226.

isotherms and pore radius distribution plots are given in the Supporting Information. The AC, S800, and A800 samples had similar particle size distributions of 3–70 μm.

The data in Table 1 show that as expected all of the Starbon® materials have higher total pore volumes than AC, but much lower micropore volumes indicating that they are predominantly mesoporous materials. Thus, whereas 73 % of the pores in AC are micropores, only 8–32 % of the pores in Starbon® are micropores. This is also reflected in the average pore radius data which for starch-derived Starbons® are an order of magnitude greater than for AC and for alginic acid-derived Starbons® are three to four times greater than for AC. The Brunauer–Emmett–Teller (BET) surface areas for Starbons® increase up to pyrolysis temperatures of 800 °C and then decrease at higher pyrolysis temperatures. This is consistent with dehydration and expulsion of steam at lower temperatures creating pores whilst at higher temperatures, partial graphitization reduces the pore sizes and hence the surface area. The adsorption isotherms showed that the pores in starch-derived Starbons® were disordered slit-shaped (H3-type isotherm according to IUPAC classification), whilst those in alginic acid–based Starbons® were interconnected ink-bottle shaped (H2-type isotherm).[10]

The CO_2 adsorption properties of the powdered carbonaceous materials were measured under pressure-swing conditions. The materials were first dried (16 hours at 110 °C, then cooled under vacuum), then subjected to five cycles of pressurize to 5 or 10 bar with CO_2 for 30 minutes, then subject to vacuum at room temperature until the mass had dropped to the value recorded after drying. The mass difference between the end of the pressurization and vacuum steps was used to calculate the number of mmols of CO_2 adsorbed per gram of sample. Figure 1 shows the average data (over the five cycles) obtained when the samples were pressurized to 5 bar (for 10 bar data see the Supporting Information). The CO_2 adsorbance obtained for AC (2.0 mmol $CO_2\,g^{-1}$) was in good agreement with that reported in the literature (2.1 mmol $CO_2\,g^{-1}$).[11]

It is apparent from Figure 1 that some of the Starbon® samples could outperform the CO_2 adsorption capacity of AC by up to 50 % (and by up to 65 % at 10 bar CO_2 pressure). For

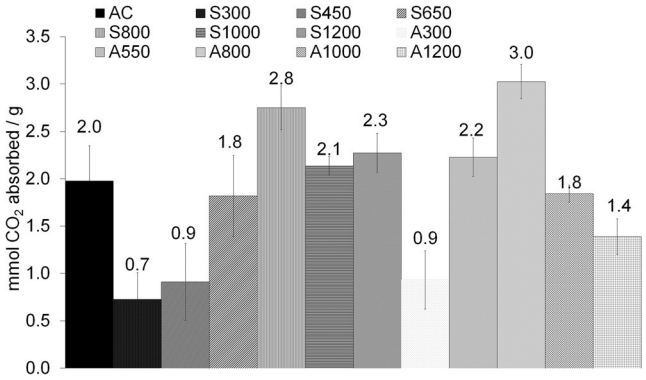

Figure 1. CO_2 adsorption data for powdered AC and Starbon® materials. The data given is the average of five measurements and the error bars represent the highest and lowest measurements for each material.

both starch- and alginic acid-derived Starbons® the optimal results were obtained using material which had been carbonized at 800 °C and corresponds to the material with the highest total surface area and smallest average pore radius (Table 1). Materials which had been carbonized at low temperatures (300–500 °C) performed very poorly, whilst material which had been carbonized at 650 °C had a similar CO_2 adsorption capability to AC. The decrease in CO_2 adsorption capacity on materials pre-treated above 800 °C was much more pronounced for alginic acid-based materials than for those based on starch. The rates of adsorption (at 5 and 10 bar CO_2 pressure) and desorption (at atmospheric pressure) were also determined (data in the Supporting Information) for AC, S800 and A800 and showed no significant differences between the three materials. At 5 bar CO_2 pressure, the materials were all saturated in 30 minutes whilst at 10 bar pressure, saturation occurred in 10 minutes. When left standing exposed to the atmosphere, complete loss of CO_2 occurred by a first order process over 20 minutes. These results show that the data presented in Figure 1 represent equilibrium adsorption data rather than any kinetic difference between the samples. They also show that S800 and optimally A800 have improved CO_2 adsorption capacities compared to AC whilst retaining the favorable rates of adsorption and desorption associated with AC. Since A800 was the optimal material for CO_2 adsorption, its reusability was further investigated and no significant loss of activity was seen over 15 cycles of pressure swing CO_2 capture and release (data in the Supporting Information).

To investigate the nature of the CO_2 adsorption by the Starbons®, the enthalpy of adsorption at 308 K of all of the materials was measured on a simultaneous thermal analyzer (STA) capable of simultaneously measuring mass and heat flow changes during adsorption and desorption phenomena allowing direct measurement of the heat of adsorption as the ratio of these two parameters. This approach is more accurate than estimation of isosteric heat of adsorption based on adsorption isotherms.[12] The data for S800 (which adsorbed the most CO_2 under these constant pressure, gas-composition swing conditions) are shown in Figure 2 (see the Supporting Information for data for other samples). The powdered sample was alternately exposed to a flow of pure N_2 and pure CO_2 and Figure 2 shows that the CO_2 adsorption process on Starbon® materials is completely reversibly at constant temperature and pressure as the gas composition changes. The rate of CO_2 adsorption and desorption is clearly also extremely rapid under these conditions. The sample mass changes allow the CO_2 adsorption to be determined at constant pressure and the same qualitative trend was observed as for the data in Figure 1, with the starch and alginic acid derived Starbons® prepared at 800 °C having the highest CO_2 adsorptions (data in the Supporting Information).

Figure 3 shows the resulting adsorption enthalpies obtained for each of the materials. All the materials have CO_2 adsorption enthalpies in the range of −14 to −22 kJ mol^{-1}(CO_2). These are in between values of heat of carbon dioxide vaporization (10.3 kJ mol^{-1})[13] and sublimation (26.1 kJ mol^{-1})[14] and indicate that for all of these

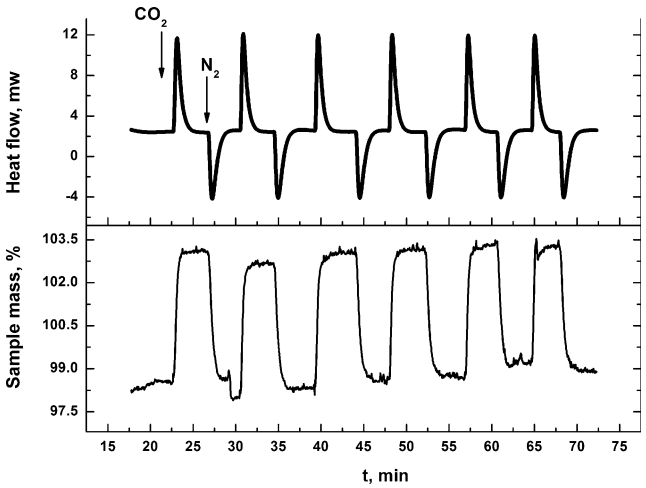

Figure 2. STA plots of mass and heat flow change during six cycles of CO_2 adsorption and desorption using powdered S800 at 308 K. The mass increases and positive heat flows coincide with the gas flow being changed from 100% N_2 to 100% CO_2. The mass decreases and negative heat flows coincide with the gas flow being changed back to 100% N_2.

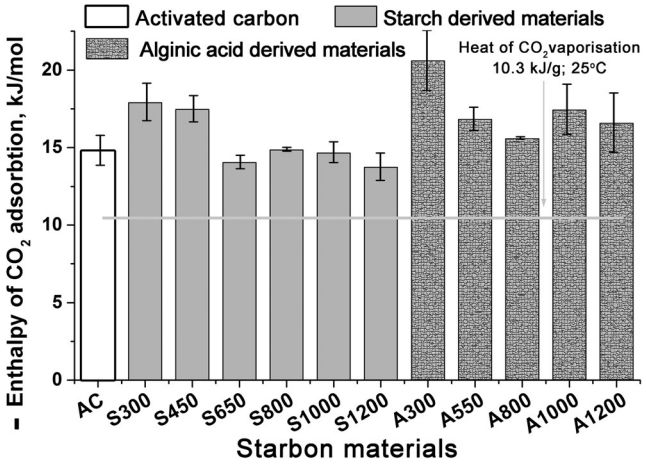

Figure 3. Enthalpies of CO_2 adsorption for powdered AC and Starbon® materials at 308 K. The data given is the average of six adsorption and desorption cycles with error bars based on the standard deviations.

materials (including activated carbon), CO_2 physisorption is the predominant adsorption mechanism. The Starbon® materials prepared at low carbonization temperatures (S300, S450, A300) had CO_2 adsorption enthalpies which were rather more negative (-18 to -21 kJ mol^{-1}(CO_2)) than the other materials and this may indicate,that for these materials, a small amount of CO_2 is chemisorbed to oxygen-containing groups which have survived the low temperature carbonization (see the Supporting Information).

Combining the data in Figure 2 and Figure 3, it is apparent that Starbon® materials can physisorb far more CO_2 than can be physisorbed by AC which is proposed to be a result of a significantly higher entropy of adsorption associated with the larger degree of freedom of CO_2 molecules adsorbed on the surface of Starbon®. In other words, CO_2 molecules adsorbed on the Starbon® surface are less restricted and have higher mobility than CO_2 molecules adsorbed on the AC surface.[14] This phenomenon could be partially related to differences in pore structure distribution of these two different types of materials and to the larger micro-/mesopore interface for Starbon materials. The most active Starbon® materials (S800 and A800) have the same micropore volumes as that of AC (0.4 cm^3 g^{-1}; see Table 1), so the additional physisorbed CO_2 must be associated with their mesoporous networks. The AC and Starbon® materials possess a range of micropore and mesopore volumes as detailed in Table 1, so the STA and porosimetry data was further analyzed to identify the key Starbon® textural parameters that control CO_2 adsorption. Application of the partial least squares regression approach (Figure 4) showed that the CO_2 adsorption is not affected by the mesopore volume, but does depend on the micropore volume and the product of the micropore and mesopore volumes and could be fitted to Equation (1) with an R^2 value of 0.98 (Figure 4). This indicates that the CO_2 is being physisorbed into the micropores, most of which are only accessible through mesopores and it is this greater accessibility of the micropores that is responsible for the enhanced CO_2 adsorption of the Starbon® materials.

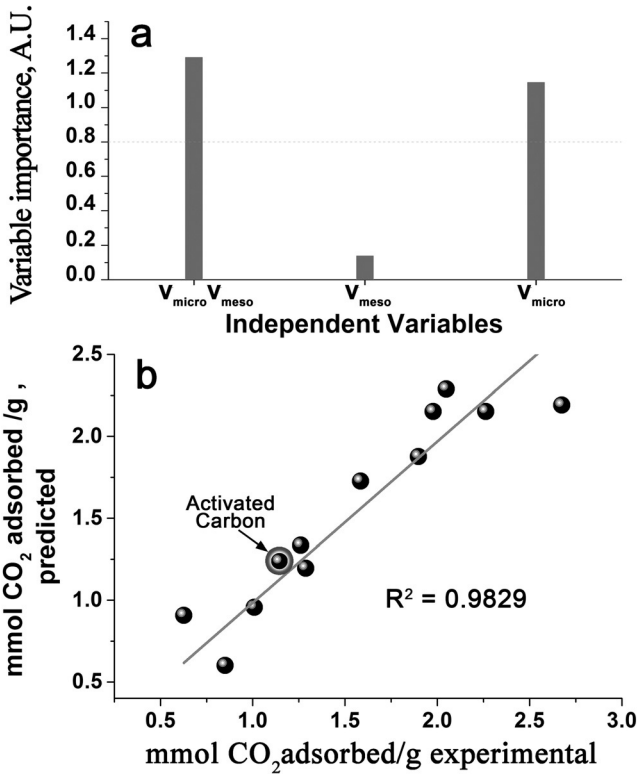

Figure 4. a) Analysis of the relative importance of micropore volume (V_{micro}), mesopore volume (V_{meso}) and the product of V_{micro} and V_{meso} in CO_2 adsorption by AC and Starbons®. b) The correlation between CO_2 adsorption data obtained from experiment and estimated from the mathematical model.

$$M_{ads}^{CO_2} = 0.095 + 2.10 * V_{micro} + 3.51 * V_{micro} * V_{meso} \quad (1)$$

The two most active mesoporous materials (S800 and A800) were selected along with AC to study the selectivity for CO_2 versus N_2 adsorption at both 298 and 323 K using porosimetry to measure the mass of gas adsorbed at pressures of 0–1 bar. Figure 5 shows the results obtained for powdered S800 (see the Supporting Information for other adsorption isotherms). As shown in Table 2, both S800 and A800, showed

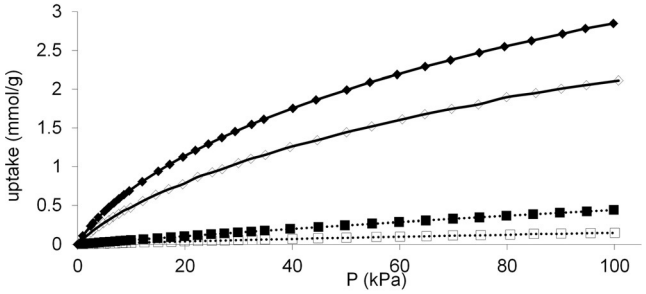

Figure 5. CO_2 and N_2 adsorption isotherms for S800. Solid lines: CO_2 adsorption and dotted lines: N_2 adsorption. Full symbols 298 K, empty symbols 323 K.

Table 2: Selectivities for CO_2 adsorption versus N_2 adsorption.

Material	*T* [K]	CO_2/N_2 selectivity
AC	298	5.4
AC	323	4.0
S800	298	14.0
S800	323	20.3
A800	298	14.8
A800	323	14.4

much greater selectivity for CO_2 adsorption than N_2 adsorption (between 14:1 and 20:1) compared to AC (between 4:1 and 5.4:1). Notably, whereas for AC the selectivity decreases from 5.4:1 to 4:1 as the temperature is raised from 298 to 323 K, for S800 and A800 the selectivity remains over 14:1 at 323 K which is the approximate temperature of flue gas and hence the preferred temperature for CO_2 separation within a carbon-capture unit.

Additional experiments were carried out with CO_2/N_2 gas mixtures using STA to investigate the selective adsorption of CO_2 at 298 K and 1 bar total gas pressure (data in the Supporting Information). Under these conditions, AC showed its maximum CO_2 adsorption at all gas compositions containing at least 50 % CO_2, whilst S800 and A800 both showed the maximum CO_2 adsorption for all gas compositions containing at least 25 % CO_2. Thus, the enhanced CO_2 selectivity seen with Starbon® materials is retained when mixtures of CO_2 and N_2 are present.

Since CO_2 in flue gas is saturated with water vapor, the effect of water on the adsorption of CO_2 was investigated at 298 K by STA using CO_2 which had been pre-saturated with water. Under these conditions, there was a 10–20 % reduction in the CO_2 adsorption capacity of powdered AC, S800, and A800, but the capacity of A800 diminished the least and the Starbon® materials maintained their advantage over AC. Water adsorption isotherms were obtained for AC, S800 and A800. The adsorption of water at $P/P_0 = 0.7$ was also investigated for the starch derived Starbons® and was found to be very low (0.08 mmol $H_2O\,g^{-1}$ for S1000 to 0.3 for S300 mmol $H_2O\,g^{-1}$). (Data given in the Supporting Information.)

In contrast to established understanding, mesoporous carbons have been shown to possess superior CO_2 adsorption properties to microporous activated carbon. Both the amount of CO_2 adsorbed and the selectivity for CO_2 adsorption rather than N_2 adsorption are improved, giving the materials potential applications in carbon capture from power station flue gases. Thermodynamic measurements indicate that CO_2 is captured by a physisorption mechanism which involves both direct and indirect (through mesopores) access to the micropores within the material. This opens a new approach to design efficient adsorbents which are optimal for CO_2 separation. Such a technology could be based on controlling the micro/meso porosities of carbonaceous materials including screening of different precursors, methods for their carbonization and chemical activation of the mesoporous carbon. Furthermore, the low adsorption enthalpy associated with CO_2 physisorption means that the process is rapidly reversible without requiring large energy input, so that CO_2 capture and release can occur under pressure swing rather than temperature swing conditions. Whilst MOFs and MOF-hybrid materials have been shown to exhibit higher CO_2 adsorptions (up to 4.23 mmol $CO_2\,g^{-1}$ at ambient temperature and pressure),[6f] this is at the expense of more complex and expensive syntheses and slower adsorption and desorption kinetics.

Acknowledgements

The authors thank Programa Operativo FSE 2007-2013 Castilla-La Mancha for funding a fellowship to GD. PSS gratefully acknowledges the Spanish Ministry Economy and Competitivity (MINECO) for a Ramón *y* Cajal fellowship (grant number RYC-2014-16759), a research project (grant number CTQ2014-52899-R) and a proyecto de I + D + I *para* jóvenes investigadores (grant number MAT2014-59674-JIN). JACO acknowledges financial support from the Plan Propio de la Universidad de Castilla-La Mancha.

Keywords: adsorption · carbon dioxide capture · carbon materials · mesoporous materials · separation

How to cite: *Angew. Chem. Int. Ed.* **2016**, *55*, 9173–9177
Angew. Chem. **2016**, *128*, 9319–9323

[1] For reviews see: a) R. Thiruvenkatachari, S. Su, H. An, X. Yu, *Prog. Energy Combust. Sci.* **2009**, *35*, 438–455; b) R. Notz, I. Tönnies, N. McCann, G. Scheffknecht, H. Hasse, *Chem. Eng. Technol.* **2011**, *34*, 163–172; c) J. Oexmann, A. Kather, S. Linnenberg, U. Liebenthal, *Greenhouse Gases Sci. Technol.* **2012**, *2*, 80–98; d) M. Zaman, J. H. Lee, *Korean J. Chem. Eng.* **2013**, *30*, 1497–1526.

[2] a) R. W. Baker, K. Lokhandwala, *Ind. Eng. Chem. Res.* **2008**, *47*, 2109–2121; b) Z. Xiang, X. Zhou, C. Zhou, S. Zhong, X. He, C.

Qin, D. Cao, *J. Mater. Chem.* **2012**, *22*, 22663 – 22669; c) S. Chaemchuen, N. A. Kabir, K. Zhou, F. Verpoort, *Chem. Soc. Rev.* **2013**, *42*, 9304 – 9332.

[3] For reviews see: a) S. Choi, J. H. Drese, C. W. Jones, *ChemSusChem* **2009**, *2*, 796 – 854; b) D. M. D'Alessandro, B. Smit, J. R. Long, *Angew. Chem. Int. Ed.* **2010**, *49*, 6058 – 6082; *Angew. Chem.* **2010**, *122*, 6194 – 6219; c) Y.-S. Bae, R. Q. Snurr, *Angew. Chem. Int. Ed.* **2011**, *50*, 11586 – 11596; *Angew. Chem.* **2011**, *123*, 11790 – 11801; d) Q. Wang, J. Luo, Z. Zhong, A. Borgna, *Energy Environ. Sci.* **2011**, *4*, 42 – 55; e) B. P. Spigarelli, S. K. Kawatra, *J. CO2 Util.* **2013**, *1*, 69 – 87.

[4] a) W. Gao, D. Butler, D. L. Tomasko, *Langmuir* **2004**, *20*, 8083 – 8089; b) R. V. Siriwardane, M.-S. Shen, E. P. Fisher, *Energy Fuels* **2005**, *19*, 1153 – 1159; c) K. S. Walton, M. B. Abney, M. D. LeVan, *Microporous Mesoporous Mater.* **2006**, *91*, 78 – 84; d) P. D. Jadhav, R. V. Chatti, R. B. Biniwale, N. K. Labhsetwar, S. Devotta, S. S. Rayalu, *Energy Fuels* **2007**, *21*, 3555 – 3559; e) F. N. Ridha, Y. Yang, P. A. Webley, *Microporous Mesoporous Mater.* **2009**, *117*, 497 – 507; f) A. Zukal, I. Dominguez, J. Mayerová, J. Čejka, *Langmuir* **2009**, *25*, 10314 – 10321; g) H. Deng, H. Yi, X. Tang, Q. Yu, P. Ning, L. Yang, *Chem. Eng. J.* **2012**, *188*, 77 – 85.

[5] a) R. V. Siriwardane, M.-S. Shen, E. P. Fisher, J. A. Poston, *Energy Fuels* **2001**, *15*, 279 – 284; b) J. Przepiórski, M. Skrodzewicz, A. W. Morawski, *Appl. Surf. Sci.* **2004**, *225*, 235 – 242; c) S. Himeno, T. Komatsu, S. Fujita, *J. Chem. Eng. Data* **2005**, *50*, 369 – 376; d) P. J. M. Carrott, I. P. P. Cansado, M. M. L. Ribeiro Carrott, *Appl. Surf. Sci.* **2006**, *252*, 5948 – 5962.

[6] For reviews see: a) Z. Xiang, D. Cao, J. Lan, W. Wang, D. P. Broom, *Energy Environ. Sci.* **2010**, *3*, 1469 – 1487; b) J.-R. Li, Y. Ma, M. C. McCarthy, J. Sculley, J. Yu, H.-K. Jeong, P. B. Balbuena, H.-C. Zhou, *Coord. Chem. Rev.* **2011**, *255*, 1791 – 1823; c) G. Férey, C. Serre, T. Devic, G. Maurin, H. Jobic, P. L. Llewellyn, G. De Weireld, A. Vimont, M. Daturi, J.-S. Chang, *Chem. Soc. Rev.* **2011**, *40*, 550 – 562; d) K. Kenji Sumida, D. L. Rogow, J. A. Mason, T. M. McDonald, E. D. Bloch, Z. R. Herm, T.-H. Bae, J. R. Long, *Chem. Rev.* **2012**, *112*, 724 – 781; e) Z. Zhang, Y. Zhao, Q. Gong, Z. Li, J. Li, *Chem. Commun.* **2013**, *49*, 653 – 661; f) Z. Zhang, Z.-Z. Yao, S. Xiang, B. Chen, *Energy Environ. Sci.* **2014**, *7*, 2868 – 2899.

[7] a) V. L. Budarin, J. H. Clark, J. J. E. Hardy, R. Luque, K. Milkowski, S. T. Tavener, A. J. Wilson, *Angew. Chem. Int. Ed.* **2006**, *45*, 3782 – 3786; *Angew. Chem.* **2006**, *118*, 3866 – 3870; b) R. J. White, V. L. Budarin, J. H. Clark, *ChemSusChem* **2008**, *1*, 408 – 411; c) R. J. White, C. Antonio, V. L. Budarin, E. Bergström, J. Thomas-Oates, J. H. Clark, *Adv. Funct. Mater.* **2010**, *20*, 1834 – 1841; d) M.-M. Titirici, R. J. White, N. Brun, V. L. Budarin, D. S. Su, F. del Monte, J. H. Clark, M. J. MacLachlang, *Chem. Soc. Rev.* **2015**, *44*, 250 – 290.

[8] a) V. Presser, J. McDonough, S.-H. Yeon, Y. Gogotsi, *Energy Environ. Sci.* **2011**, *4*, 3059 – 3066; b) A. Samanta, A. Zhao, G. K. H. Shimizu, P. Sarkar, R. Gupta, *Ind. Eng. Chem. Res.* **2012**, *51*, 1438 – 1463; c) A.-H. Lu, G. P. Hao, *Annu. Rep. Prog. Chem. Sect. A* **2013**, *109*, 484 – 503; d) Y. Zhao, X. Liu, Y. Han, *RSC Adv.* **2015**, *5*, 30310 – 30330.

[9] The amount of CO_2 adsorbed is known not to depend on physical parameters such as surface area, pore volume, and micropore volume which may differ between activated carbons. Hence, Norit activated charcoal is representative of all microporous carbons: B. Guo, L. Chang, K. Xie, *J. Nat. Gas. Chem.* **2006**, *15*, 223 – 229.

[10] a) K. S. W. Sing, D. H. Everett, R. A. W. Haul, L. Moscou, R. A. Pierotti, J. Rouquérol, T. Siemieniewska, *Pure Appl. Chem.* **1985**, *57*, 603 – 619; b) F. Rojas, I. Kornhauser, C. Felipe, J. M. Esparza, S. Cordero, A. Domínguez, J. L. Riccardo, *Phys. Chem. Chem. Phys.* **2002**, *4*, 2346 – 2355.

[11] W. Travis, S. Gadipelli, Z. Guo, *RSC Adv.* **2015**, *5*, 29558 – 29562.

[12] D. Wu, J. J. Gassensmith, D. Gouvêa, S. Ushakov, J. F. Stoddart, A. Navrotsky, *J. Am. Chem. Soc.* **2013**, *135*, 6790 – 6793.

[13] K. H. Yung, *J. Phys. Chem.* **1995**, *99*, 12021 – 12024.

[14] http://webbook.nist.gov/cgi/cbook.cgi?ID = C124389&Mask = 4#Thermo-Phase.

Received: March 3, 2016
Revised: May 31, 2016
Published online: June 23, 2016

